Electronic Supplementary Material (ESI) for Chemical Communications.

Supporting Information

Crystal Structure and Orientation of Organic Semiconductor Thin Films by Microcrystal Electron Diffraction and Grazing-Incidence Wide-angle X-ray Scattering

Andrew M. Levine[a,b,c], Guanhong Bu[d,e], Sankarsan Biswas[a,b,c], Esther H. R. Tsai*[f], Adam B. Braunschweig*[a,b,c] , and Brent L. Nannenga*[d,e]

[a]Nanoscience Initiative, Advanced Science Research Center, Graduate Center, City University of New York, 85 St. Nicholas Terrace, New York, NY 10031, USA.
[b]Department of Chemistry, Hunter College, 695 Park Avenue, New York, NY 10065, USA.
[c]PhD Program in Chemistry, Graduate Center, City University of New York, 365 5th Avenue, New York, NY 10016, USA.
[d]Chemical Engineering, School for Engineering of Matter, Transport, and Energy, Arizona State University, Tempe, AZ 85287, USA.
[e]Center for Applied Structural Discovery, The Biodesign Institute, Arizona State University, Tempe, AZ, USA.
[f]Center for Functional Nanomaterials, Brookhaven National Laboratory, Upton, NY 11973, USA.

Table of Contents

1. Synthesis

dPyr PDI[1], dCN NDI[2], and dDPP[3] were synthesized using previously reported procedures. All reagents and starting materials were purchased from MilliporeSigma or VWR and used without further purification unless otherwise noted. Thin-layer chromatography was carried out using aluminum sheets precoated with silica gel 60 (EMD 40 - 60 mm, 230 - 400 mesh with 254 nm dye). Silica gel (BDH 60 Å) was used for flash column chromatography. All solvents were dried prior to use, and all reactions were carried out under N_2 atmosphere using standard Schlenk techniques. Deuterated solvents were purchased from Cambridge Isotope Laboratories Inc. and used as received. Proton NMR spectra were obtained on Bruker AVANCE 300 MHz spectrometer and all spectroscopic data was consistent with the previous reports.

2. MicroED Sample Preparation

3 µL of 10 mM toluene solutions of each compound were dropped onto continuous carbon grids [Electron Microscope Sciences CF400-CU] for 1 min and then wicked dry from the grid edge using filter paper [Whatman Cat No 1001-070]. Grids were subsequently placed into autoloader cartridges under liquid N_2 and loaded into a Titan Krios cryo-TEM equipped with a CETA D detector for MicroED analysis.

3. MicroED Data Collection

Standard MicroED Data collection procedures were used[4], with slight modifications as described below. With the search mode of the microscope's low-dose settings, low magnification (LM mode, ~600x) was used to initially screen the quality of the grids and identify promising nanocrystals on the grid. Promising nanocrystals were those which were small and well-separated from other crystals on the grid (See circled crystals in Figures 1A, and S1 for representative nanocrystals). Upon identifying nanocrystals, initial diffraction patterns were collected by switching the cryo-TEM into diffraction mode by using "exposure" mode in the low-dose settings and acquiring an initial diffraction pattern. If this initial diffraction pattern showed high quality diffraction (defined as patterns showing clear and sharp diffraction spots that extend to high-resolution), the microscope was put back into search mode and the maximum possible tilt range of the stage was determined for that crystal by tilting the stage and ensuring the crystal remains centered (correct eucentric height is critical) and no other crystals or grid bars overlap with the crystal. For all samples it was found that the best diffracting nanocrystals were on the order of 0.5-1.5 µm and 0.2-0.5 µm for length and width, and less than approximately 0.1 µm in thickness. The selected area aperture size is chosen such that the entire crystal is within the aperture while also minimizing area the surrounding the crystal. MicroED data sets are collected by continuously rotating the crystal in the beam as the CETA D camera is continuously acquiring diffraction images.

Table S1. Data collection and refinement statistics for the three organic semiconductor samples.

	dPyr PDI	**dCN NDI**	**dDPP**
Data collection			
Excitation Voltage	300 kV	300 kV	300 kV
Wavelength (Å)	0.019687	0.019687	0.019687
Number of crystals	3	8	7
Data Processing			
Space group	Cc	$P2_1/c$	$P2_1/n$
Unit cell length a, b, c (Å)	22.05, 10.76, 9.34	8.09, 6.39, 11.63	15.09, 19.55, 34.77
Angles α, β, ɣ (°)	90.000, 101.287, 90.000	90.000, 104.711, 90.000	90.000, 94.627, 90.000
Resolution (Å)	0.60	0.57	0.90
Measured reflections	23,894	27,418	134,916
Unique reflections	4,661	2,512	14,926
Redundancy	5.1	10.9	9.0
R_{obs} (%)	17.4 (41.2)	19.2 (43.8)	28.0 (129.0)
R_{meas} (%)	19.0 (52.1)	19.9 (53.3)	29.7 (146.7)
I/σ_I	4.48 (1.14)	6.81 (0.98)	4.15 (0.66)
$CC_{1/2}$ (%)	99.4 (45.5)	97.7 (79.4)	97.7 (20.5)
Completeness (%)	84.7 (41.8)	71.5 (49.0)	97.5 (77.3)
Structure Refinement			
Stoichiometric Formula	$C_{32}H_{24}N_4O_4$	$C_{16}H_4N_4O_4$	$C_{54}H_{70}N_8O_6S_2$
R1	0.2355 (0.1991)	0.1690 (0.1376)	0.2908 (0.2350)
wR2	0.5085	0.3919	0.5555
GooF	1.423	1.141	1.813

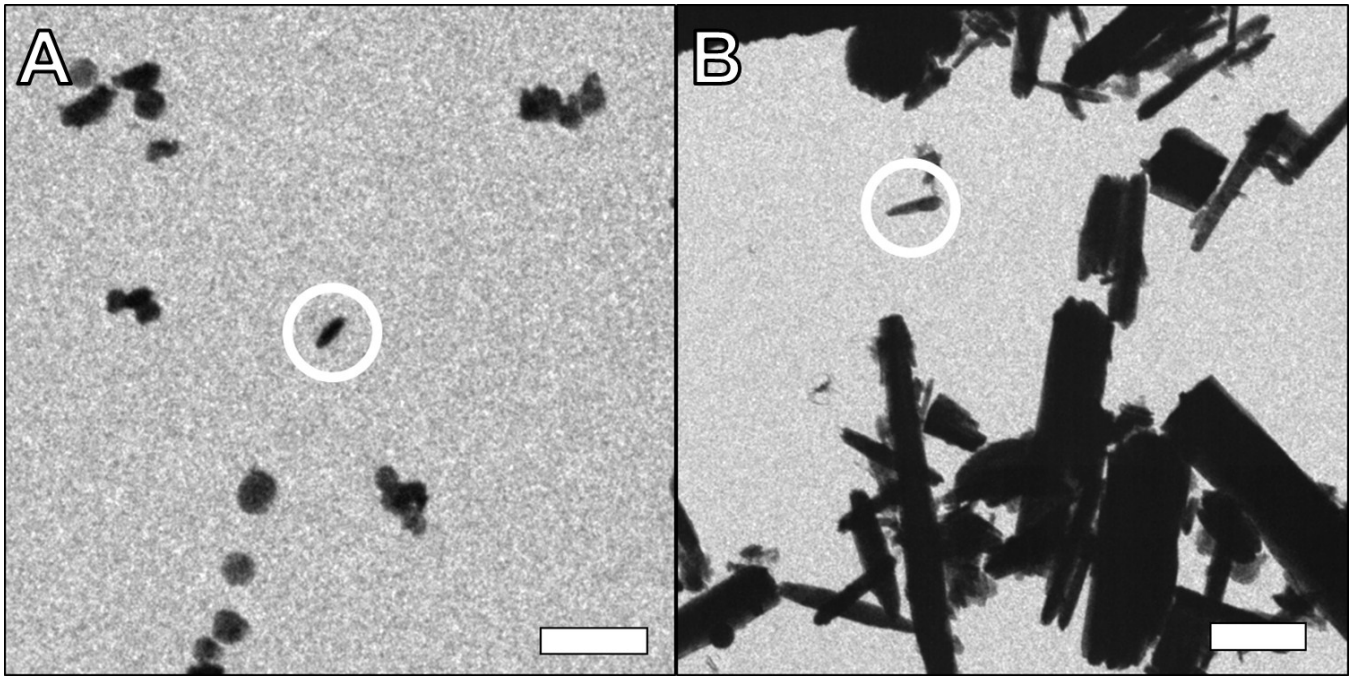

Figure S1. Example (A) dCN NDI and (B) dDPP crystals under low magnification view on the EM grid. Representative crystals used for diffraction are circled. Scale bars represent 2 μm.

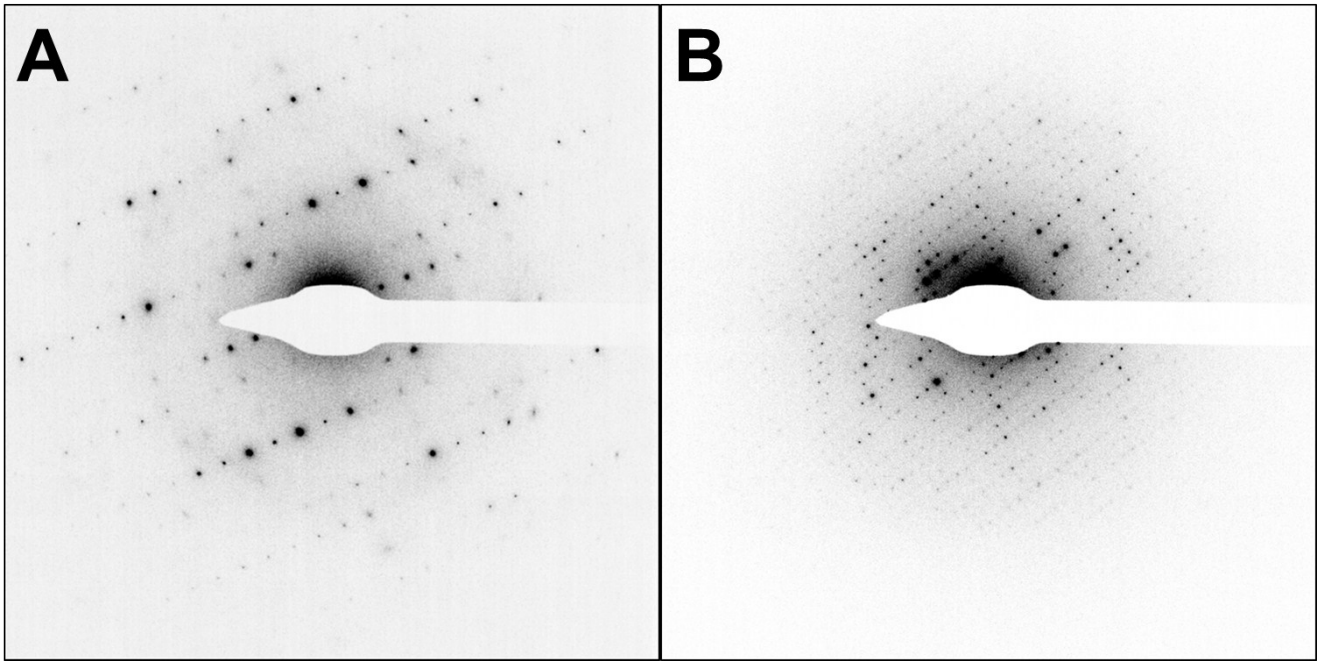

Figure S2. Example diffraction patterns of (A) dCN NDI, which extends beyond 0.6 Å, and (B) dDPP, which extends to 0.90 Å. The edge of the detector is approximately 0.65Å in A and B.

4. MicroED Data Processing

MicroED data were converted from MRC to SMV format for further data processing[5], and the processing and refinement procedures followed standard workflows for MicroED [6]. The data sets were indexed, integrated, and scaled using XDS[7]. Structures were solved by direct methods in SHELXT[8] and refined using the ShelXle[9] graphical interface for SHELXL[10].

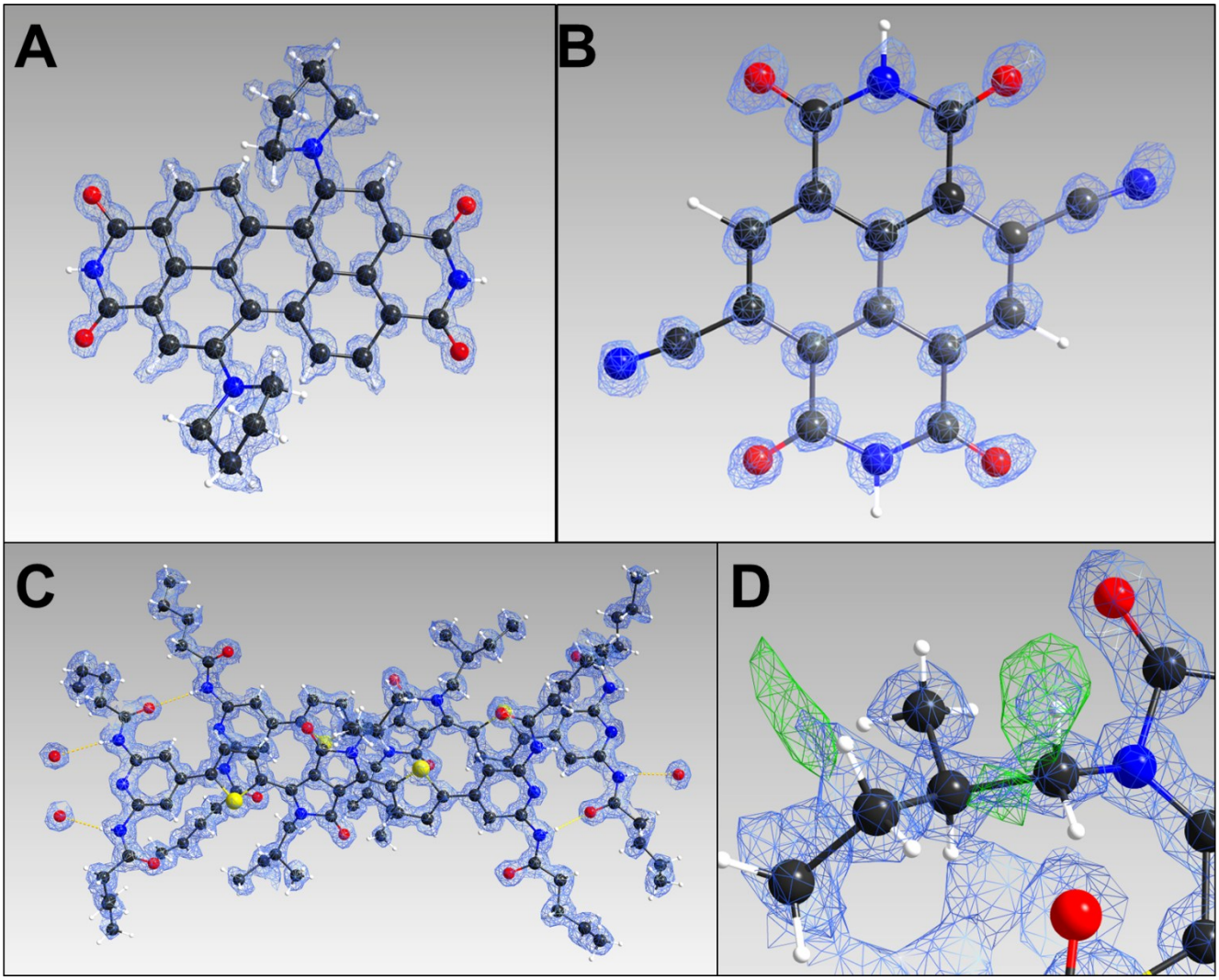

Figure S3. F_o density maps of (A) dPyr PDI (0.60 Å resolution), (B) dCN NDI (0.57 Å resolution), and (C,D) dDPP (0.90 Å resolution) all contoured at 1.5σ. Models and maps were visualized in ShelxLe.

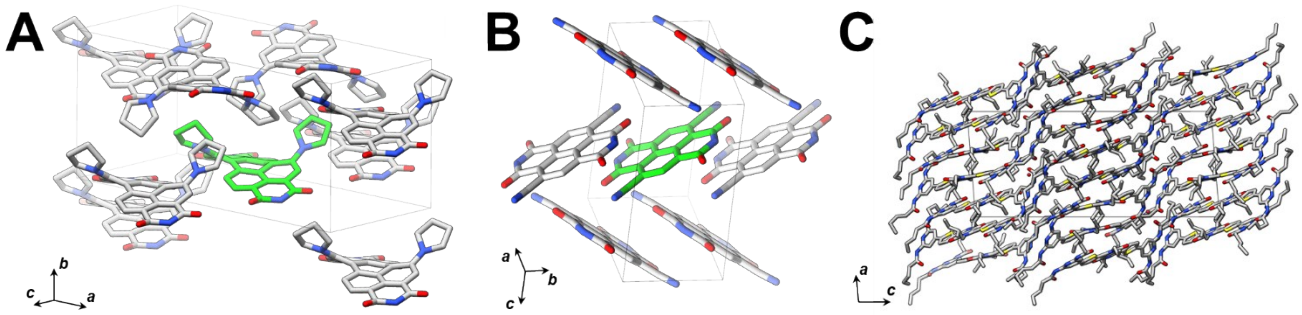

Figure S4. Additional view of the solved (A) dPyr PDI, (B) dCN NDI, and (C) dDPP crystal structures from MicroED data.

5. GIWAXS

Glass substrates were cleaned by sonicating in detergent water for 10 min, acetone for 10 min, isopropyl alcohol for 10 min, and then plasma cleaning [Harrick Plasma Cleaner PDC-32 G] for 10 min. Thin films of dPyr PDI and dDPP films were prepared for GIWAXS measurements by drop casting 60 µL of 10 mM toluene solutions onto clean glass slides and allowing them to dry in air. dCN NDI was thermally evaporated using a RADAK I Thermal Evaporator at a rate of 0.1 Å/s for 1 nm and then increased to 0.5 Å/s for a total of 40 nm.

GIWAXS experiments were performed at beamline 12-ID SMI at the National Synchrotron Light Source II (NSLS-II) at Brookhaven National Laboratory, NY, USA. Samples on glass substrates were illuminated by an X-ray beam at wavelength 0.77 Å and with beam-size horizontally 200 um and vertically 30 um in a grazing incident geometry with an incident angle of 0.1 degree. Scattering patterns were recorded by a Pilatus300K detector 0.2739 m downstream of the sample. The detector scanned across the q-range needed for the study and multiple scattering patterns were stitched together to obtain the final scattering data, shown for example in Fig. 1E and Fig. S5. Integrated 1D intensity plots versus the scattering vector q were obtained through in-house beamline analysis software.

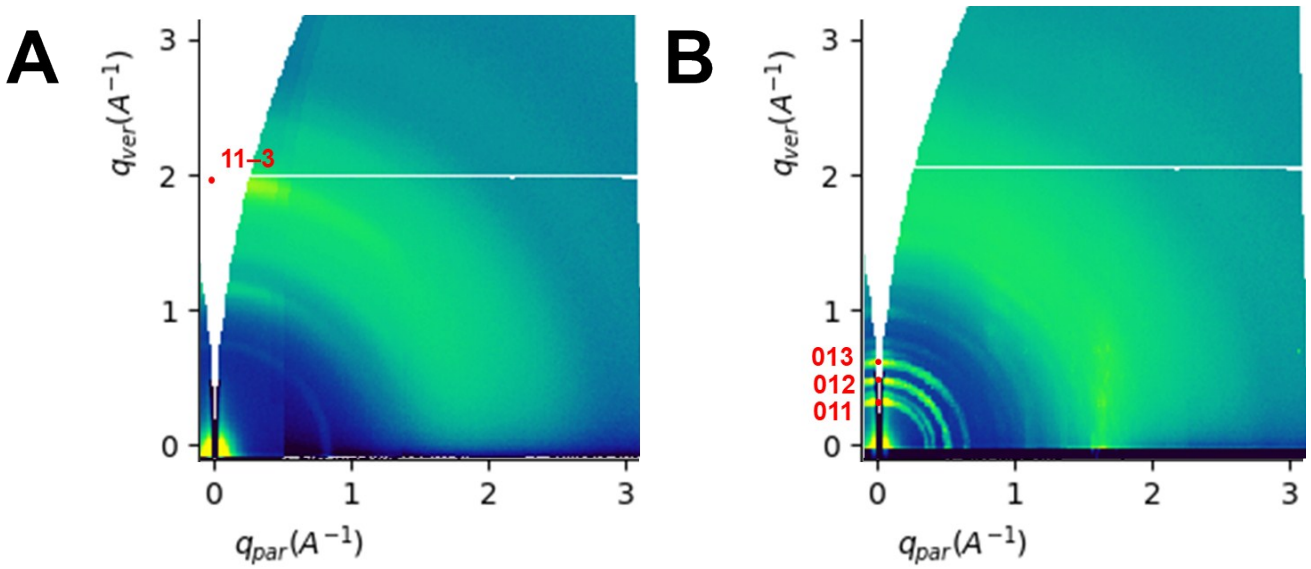

Figure S5. Q-space generated from GIWAXS data for (A) dCN NDI and (B) dDPP.

Given the crystal structures from MicroED, GIWAXS scattering patterns were indexed with in-house analysis tools to determine the molecule orientations in thin films.[11] The GIWAXS data with indexing provides an estimation of the molecular orientation relative to the substrate.

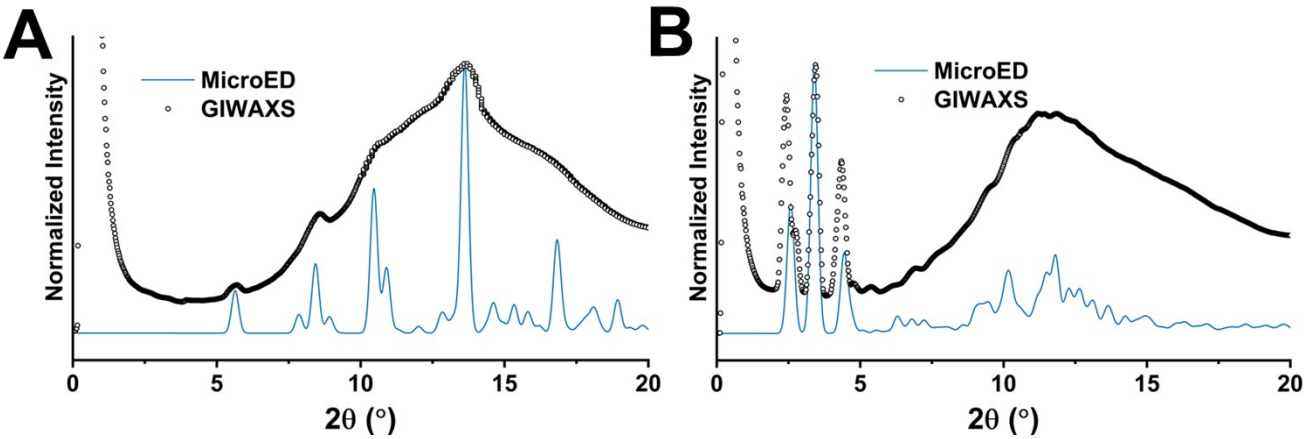

Figure S6. Comparison of MicroED generated powder pattern and GIWAXS data for (A) dCN NDI and (B) dDPP.

6. References

1. L. M. Smieska, Z. Li, D. Ley, A. B. Braunschweig and J. A. Marohn, *Chem. Mater.*, 2016, **28**, 813-820.
2. G. S. Vadehra, R. P. Maloney, M. A. Garcia-Garibay and B. Dunn, *Chem. Mater.*, 2014, **26**, 7151-7157.

3. A. M. Levine, C. Schierl, B. S. Basel, M. Ahmed, B. A. Camargo, D. M. Guldi and A. B. Braunschweig, *J. Phys. Chem. C*, 2019, **123**, 1587-1595.
4. B. L. Nannenga and T. Gonen, *Nat. Methods*, 2019, **16**, 369-379.
5. J. Hattne, M. W. Martynowycz and T. Gonen, *bioRxiv*, 2019, DOI: 10.1101/615484, 615484.
6. B. L. Nannenga, *Struct Dyn*, 2020, **7**, 014304.
7. W. Kabsch, *Acta Crystallogr. Sect. D. Biol. Crystallogr.*, 2010, **66**, 125-132.
8. G. M. Sheldrick, *Acta Crystallogr. Sect. A: Found. Crystallogr.*, 2015, **71**, 3-8.
9. C. B. Hubschle, G. M. Sheldrick and B. Dittrich, *J. Appl. Cryst.*, 2011, **44**, 1281-1284.
10. G. M. Sheldrick, *Acta Crystallogr. Sect. C: Cryst. Struct. Commun.*, 2015, **71**, 3-8.
11. D.-M. Smilgies and D. R. Blasini, *J. Appl. Crystallogr.*, 2007, **40**, 716-718.